Applied Catalysis B: Environmental 146 (2014) 267–273

Contents lists available at ScienceDirect

Applied Catalysis B: Environmental

journal homepage: www.elsevier.com/locate/apcatb

Conversion of glycerol into allyl alcohol over potassium-supported zirconia–iron oxide catalyst

Aya Konaka, Teruoki Tago*, Takuya Yoshikawa, Ayaka Nakamura, Takao Masuda

Research Group of Chemical Engineering, Division of Chemical Process Engineering, Faculty of Engineering, Hokkaido University, N13W8, Kita-ku, Sapporo, Hokkaido 060-8628, Japan

ARTICLE INFO

Article history:
Received 30 October 2012
Received in revised form 23 February 2013
Accepted 3 March 2013
Available online 14 March 2013

Keywords:
Biomass utilization
Glycerol conversion
Crude glycerol
Iron oxide catalyst
Allyl alcohol

ABSTRACT

The catalytic conversion of glycerol was performed with iron oxide-based catalysts for production of allyl alcohol using a fixed-bed flow reactor at 623 K under atmospheric pressure. The glycerol dehydration proceeds on acid sites of catalysts while the allyl alcohol production is assumed to be catalyzed by non-acidic sites of catalysts through a hydrogen transfer mechanism. Different alkali metals, including Na, K, Rb, and Cs were supported on ZrO_2–FeO_X and all of them gave impressively higher allyl alcohol yield and suppressed glycerol dehydration due to the reduced catalyst acidic property. K-supported ZrO_2–FeO_X (K/ZrO_2–FeO_X) was chosen for further studies, and allyl alcohol yield remarkably increased up to 27 mol% C at the K content of 3–5 mol%. Since no external hydrogen gas is supplied to the system, the hydrogen transfer mechanism should take place between the reaction of glycerol and either hydrogen atoms derived from formic acid forming during the reaction, or active hydrogen species produced from the decomposition of H_2O by ZrO_2.

Addition of Al_2O_3 to K/ZrO_2–FeO_X (K/Al_2O_3–ZrO_2–FeO_X) was examined in order to improve structure stability during the glycerol conversion. Al_2O_3 addition to the catalyst was effective to achieve higher structure stability, leading to high glycerol conversion with stable allyl alcohol yield of above 25 mol% C. Moreover, K/Al_2O_3–ZrO_2–FeO_X can be applicable to the conversion of crude glycerol which is the waste solution obtained from biodiesel production.

1. Introduction

Biodiesel, one of renewable and alternative fuels to fossil fuels, appears to be significant fuel due to depletion of fossil fuels and global warming problem [1–3]. Glycerol is produced as a main by-product in a biodiesel production which is a transesterification of triglycerides, such as vegetable oils and animal fats, and methanol [2,4]. Therefore, development of an effective utilization for glycerol is highly desired.

Conversion of glycerol into useful chemicals is widely studied [5–15]. Most of the works report on converting glycerol into acrolein [5–7], acetol [8], or 1,2- and 1,3-propanediol [9–11]. Acrolein and acetol are produced through gas-phase dehydration of glycerol over acidic catalysts including Nb_2O_5, heteropolyacids, and zeolites, and copper metal catalysts, respectively. 1,2- and 1,3-Propanediol are obtained through hydrogenolysis of glycerol over supported Ru, Rh, and Pt catalysts. Additionally, some of the works have reported recently on synthesis of allyl alcohol from glycerol which is assumed to form via hydride or hydrogen transfer mechanism [12–15]. Among these chemicals, allyl alcohol can be more useful and valuable chemical because it can be used as an important chemical intermediate in the production of resins, paints, coatings, silane coupling agents, and polymer crosslinking agents, etc. Thus, allyl alcohol is one attractive and valuable chemical that can be obtained from glycerol.

On the contrary, we have developed zirconia–iron oxide catalyst, ZrO_2–FeO_X, for the catalytic conversion of biomass resources. We have succeeded in producing phenol and ketones from tar derived from wood biomass [16–19], sewage sludge [20], and fermentation residue [21] over ZrO_2–FeO_X, in which ZrO_2 loaded on FeO_X contributes to the high catalytic performance and stability. Since ZrO_2–FeO_X works effectively on the organic compounds having hydroxyl and carboxyl groups, the catalyst is expected to be applicable to the catalytic conversion of glycerol into useful chemicals.

Using ZrO_2–FeO_X, we have succeeded in producing useful chemicals, including propylene, allyl alcohol, carboxylic acids, and ketones, from reagent glycerol [22]. These useful chemicals are expected to be produced from glycerol through two main pathways: one pathway involves the production of allyl alcohol and propylene (Pathway I), and another involves the production of carboxylic acids from acetol, followed by their ketonization (Pathway

* Corresponding author. Tel.: +81 11 706 6551; fax: +81 11 706 6552.
E-mail address: tago@eng.hokudai.ac.jp (T. Tago).

0926-3373/$ – see front matter © 2013 Elsevier B.V. All rights reserved.
http://dx.doi.org/10.1016/j.apcatb.2013.03.007

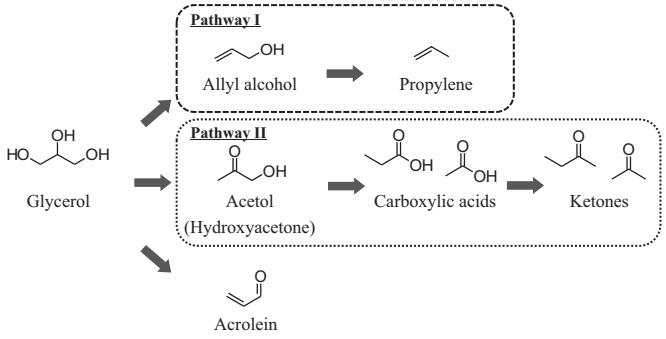

Fig. 1. Expected reaction pathways for glycerol over ZrO_2–FeO_X.

II), as shown in Fig. 1. We previously reported that the incorporation of ZrO_2 into FeO_X significantly improved the BET surface area of the catalysts; FeO_X has the surface area of 14 $m^2\,g^{-1}$ while ZrO_2–FeO_X with ZrO_2 content of 7.0 wt% has that of 56 $m^2\,g^{-1}$ [22,23]. This increase in the catalyst surface area further improved the catalytic activity for the production of the useful chemicals shown in Fig. 1. Furthermore, it was also revealed that ZrO_2–FeO_X improved the catalytic stability because ZrO_2 has an ability to produce active oxygen species from H_2O for regeneration of the consumed lattice oxygen in FeO_X [22–24]. In our previous research, ZrO_2–FeO_X was considered to have acid sites which generally promote dehydration reaction [25–27]. In order to obtain higher selectivity to the Pathway I, particularly allyl alcohol, suppressing the Pathway II and the acrolein production, which are the dehydration of glycerol, appears to be a solution to our system.

In this study, different alkali metals, including Na, K, Rb, and Cs were supported on ZrO_2–FeO_X to suppress glycerol dehydration that proceeded on the acid sites of the catalyst. Na-, K-, Rb-, and Cs-supported ZrO_2–FeO_X were used for the catalytic conversion of glycerol. K-supported ZrO_2–FeO_X was selected for the further studies and its effects of K content on the product yield and catalytic stability were investigated. Main objectives of this study are to investigate the effects of supported alkali metals on the product yield and to develop a catalyst showing high selectivity to allyl alcohol with high stability. Finally, the catalyst was applied to convert crude glycerol derived from biodiesel production to allyl alcohol.

2. Experimental

2.1. Catalyst preparation and characterization

All reagents were purchased from Wako Pure Chemical Industries (Japan). ZrO_2–FeO_X was prepared by a coprecipitation method using $Fe(NO_3)_3{\cdot}9H_2O$ and $ZrO(NO_3)_2{\cdot}2H_2O$ aqueous solutions and ammonia solution. 10 wt% ammonia solution was added by a micropump to the aqueous solution of $Fe(NO_3)_3{\cdot}9H_2O$ and $ZrO(NO_3)_2{\cdot}2H_2O$ under continuous stirring until the pH of each solutions reached pH 7 and filtered subsequently. The obtained precipitate was dried at 383 K for 24 h to obtain ZrO_2–FeO_X precursor. In our previous research [22], the effect of ZrO_2 content on product yield from glycerol was examined, in which it was revealed that ZrO_2 content of 7.0 wt% in FeO_X was appropriate. In this study, ZrO_2–FeO_X with ZrO_2 content of 7.0 wt% was used as a catalyst.

The ZrO_2–FeO_X precursor was used to prepare alkali metal-supported ZrO_2–FeO_X by an impregnation method with their content of 1.0 mol% based on the total amount of Zr and Fe. As for K, its content was varied in the range of 0–10 mol%, denoted hereafter "K[*Z*]/ZrO_2–FeO_X" where *Z* was the K content (mol%). Aqueous solution of each alkali metal nitrates was added to the ZrO_2–FeO_X precursor, stirred and dried in a vacuum at 313 K for 2 h and 333 K for 2 h. The obtained precipitate was again dried at 383 K for 24 h and finally calcined at 773 K for 2 h in an air atmosphere. The BET surface area of the representative catalyst, K[5]/ZrO_2–FeO_X, was 51 $m^2\,g^{-1}$ and its crystal phase was hematite.

K-supported Al_2O_3–ZrO_2–FeO_X, K/Al_2O_3–ZrO_2–FeO_X, was also prepared by a combination of coprecipitation and impregnation methods. Al_2O_3-ZrO_2–FeO_X precursor was first obtained by a coprecipitation method similarly to the protocols for the preparation of ZrO_2–FeO_X [23]. $Al(NO_3)_3{\cdot}9H_2O$ was used as the Al_2O_3 source. Al_2O_3 content was 10 mol% of the total amount of Al, Zr, and Fe. K was supported on Al_2O_3–ZrO_2–FeO_X by an impregnation method. The Al_2O_3–ZrO_2–FeO_X precursor and KNO_3 aqueous solution were mixed, stirred, and subsequently dried in a vacuum at 313 K for 2 h and 333 K for 2 h. The obtained precipitate was dried at 383 K for 24 h and finally calcined at 973 K for 2 h in an air atmosphere. The obtained catalyst had the BET surface area of 62 $m^2\,g^{-1}$ and the crystal phase of hematite.

The composition of the catalysts and the amount of ZrO_2 or alkali metals in the catalysts were confirmed by X-ray fluorescence analyzer (XRF Supermini; Rigaku Co. Ltd.). The surface areas of the catalysts were measured by a nitrogen adsorption and desorption method (Belsorp mini; BEL Japan, Inc.). The crystal phases of the catalysts were analyzed by an X-ray diffractometer (JDX–8020; JEOL). The acidic property of the catalysts was evaluated by the temperature-programmed desorption profile of ammonia (NH_3-TPD) method using the quadropole mass spectrometer (BEL-mass; BEL Japan, Inc.) combined with the catalyst analyzer (BEL-cat; BEL Japan, Inc.). The sample was pretreated in Ar flow at 823 K. After cooling down to 373 K, NH_3 was introduced for 30 min and the sample was subsequently heated at 10 K min^{-1} in Ar flow up to 823 K.

2.2. Catalytic conversion of glycerol

The catalytic conversion of glycerol over different catalysts was carried out in a fixed-bed flow reactor for 2–6 h at the reaction temperature of 623 K under atmospheric pressure. Catalysts were pelletized and formulated into the particle size of 300–850 μm. Nitrogen gas was introduced as a carrier gas at the flow rate of 20 cm^3/min. The values of *W*/*F*, where *W* is the amount of catalyst (g) and *F* is the flow rate of the feedstock (g h^{-1}), were varied in the range of 1–5 h to obtain similar initial glycerol conversion between each experiment. Glycerol aqueous solution was used as a feedstock and fed to the reactor with a syringe pump. Crude glycerol solution, the waste solution obtained in the process of biodiesel fuel production, was also used as a feedstock. The main source of the crude glycerol is edible vegetable oil and methanol. Potassium hydroxide, KOH, is used as a catalyst for the transesterification reaction of them to produce biodiesel fuel and glycerol.

The liquid and the gas products were collected with an ice trap and a gas pack, respectively, for every 2 h and product yields showed the average of each 2 h. The liquid products were analyzed by a gas chromatograph equipped with a flame ionization detector (GC-2014; Shimadzu Co. Ltd.) and a gas chromatograph mass (GC-17A GCMS-QP5050) equipped with a DB-Wax capillary column. The gas products were analyzed by gas chromatographs with thermal conductivity and flame ionization detectors (GC-8A; Shimadzu Co. Ltd.) equipped with activated charcoal and Porapak Q columns, respectively. The product yields were calculated based on the amount of glycerol fed to the reactor.

3. Results and discussion

3.1. Catalytic reactions over alkali metal-supported ZrO_2–FeO_X

In a biodiesel fuel production process, alkali metals such as sodium (Na) or potassium (K) hydroxides are used as catalysts in

Table 1
Product yields obtained for different alkali metal-supported ZrO_2–FeO_X. Reaction conditions: 30 wt% glycerol solution, alkali metal-supported ZrO_2–FeO_X, W/F = 3 h, reaction time=6 h.

ZrO_2–FeO_X	Glycerol conversion (%)	Product yield (mol% C)									
		Path I			Path II				Aldehydes		
		Propylene	Allyl alcohol	Path I	Acetol	Carboxylic acids	Ketones	Path II	Acrolein	Acetaldehyde	Aldehydes
–	100	5.9	13.7	19.6	1.2	21.2	9.2	31.6	6.3	3.6	9.9
Na	100	4.3	20.2	**24.5**	0.2	12.6	9.7	**22.5**	4.8	3.8	**8.6**
K	98.8	4.4	20.7	**25.1**	2.1	13.8	8.1	**24.0**	3.9	2.7	**6.6**
Rb	100	4.8	19.6	**24.4**	0.0	11.4	11.7	**23.1**	3.6	3.4	**7.0**
Cs	99.8	4.4	19.7	**24.1**	1.0	14.4	10.4	**25.8**	3.2	2.3	**5.5**

Bold values mean total product yields in each pathway shown in Fig. 1.

the transesterification reaction. Therefore, crude glycerol, a waste solution obtained in a biodiesel fuel production process, contains these alkali metal ions. In a catalytic conversion of crude glycerol, these alkali metal ions are supposed to deposit on catalyst surface. Accordingly, the effect of loading of alkali metal on product yields was investigated. ZrO_2–FeO_X and Na-, K-, Rb-, and Cs-supported ZrO_2–FeO_X were used to convert 30 wt% glycerol solution for 6 h at W/F of 3 h. Table 1 shows the product yields of the Pathway I (allyl alcohol and propylene), the Pathway II (acetol, carboxylic acids, and ketones), and aldehydes (acrolein and acetaldehyde) obtained when ZrO_2–FeO_X and different alkali metal-supported ZrO_2–FeO_X were used for the glycerol conversion.

Almost complete glycerol conversions were attained for ZrO_2–FeO_X and all alkali metal-supported ZrO_2–FeO_X, which indicated that alkali metals do not significantly influence the glycerol conversion. ZrO_2–FeO_X yielded approximately 20 mol% C of the Pathway I, 32 mol% C of the Pathway II, and 10 mol% C of aldehydes. In comparison, all alkali metal-supported ZrO_2–FeO_X showed higher product yields of the Pathway I (24–25 mol% C), and remarkably lower product yields of the Pathway II (23–26 mol% C) and aldehydes (6–8 mol% C). Interestingly, allyl alcohol yield considerably increased from 13.7 mol% C to approximately 20 mol% C.

Among the all alkali metals investigated, K was selected for the further studies because it showed relatively high Pathway I yield. Effect of K content on the dehydration of glycerol was studied. K[Z]/ZrO_2–FeO_X, where K content Z varied from 0 to 10 mol%, was used to convert 30 wt% glycerol solution for 2 h at W/F of 1 h. Fig. 2 shows the glycerol conversions and the product yields obtained for K[Z]/ZrO_2–FeO_X (Z = 0–10 mol%). The glycerol conversions maintained higher than 96% over the K content of 0–5 mol% but the further increase in K content caused a moderate drop in the conversion down to 84%. This could be explained by the coverage of the active sites of ZrO_2–FeO_X with the excessive amount of K existed on the catalyst. Notably, adding K on ZrO_2–FeO_X and the increase in its content resulted in a remarkable increase in allyl alcohol yield up to 27 mol% C at the K content of 3–5 mol%. Furthermore, the addition of K led a drastic decrease in acetol, carboxylic acids, ketones, and aldehydes yields and this trend was notable at the higher K content. Regarding the selectivity to allyl alcohol, K[5]/ZrO_2–FeO_X was concluded to be the catalyst having the most suitable K content and selected for the further studies. Furthermore, these results indicate that the glycerol dehydration, the Pathway II and the aldehydes formations, is effectively suppressed by the addition of K. Since the glycerol dehydration is considered to proceed on acid sites of catalysts, its suppression should be resulted from the decreased acidic property of the catalyst.

To confirm this, temperature-programmed desorption of ammonia (NH_3-TPD) was carried out to study the acidic properties of ZrO_2–FeO_X, K[1]/ZrO_2–FeO_X, and K[5]/ZrO_2–FeO_X. The amount of desorbed NH_3 for ZrO_2–FeO_X was approximately 0.07 mmol kg cat^{-1} while those for K[1]/ZrO_2–FeO_X and K[5]/ZrO_2–FeO_X were reduced to 0.01 mmol kg cat^{-1} or less as shown in Fig. 3. The amount of desorbed NH_3 impressively decreased with the increase in K content, which in turn resulted in the further decrease in the acidic property of the catalyst. Additionally, the peak position of the NH_3-TPD profile was shifted to the

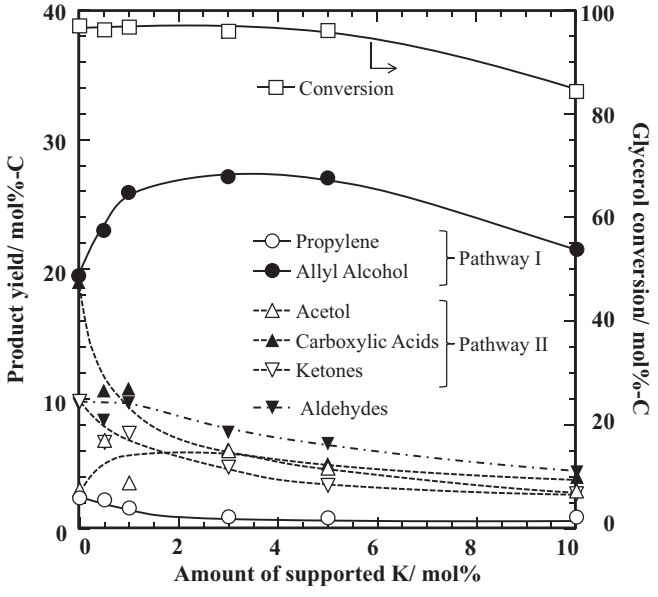

Fig. 2. Effect of K content on the product yields. Reaction conditions: 30 wt% glycerol solution, K[Z]/ZrO_2–FeO_X (Z = 0–10 mol%), W/F = 1 h, reaction time = 2 h.

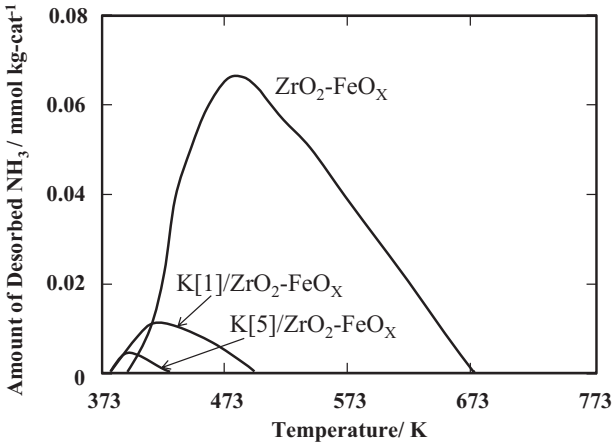

Fig. 3. NH_3-TPD profiles for ZrO_2–FeO_X, K[1]/ZrO_2–FeO_X, and K[5]/ZrO_2–FeO_X.

lower temperature as the amount of K content increased. These results indicated that the acidic property of ZrO_2–FeO_X had been lowered by the addition of K, which in turn led to the suppression of the glycerol dehydration.

The catalyst acidity is assumed to be derived from the hydroxyl groups exit on the catalyst surface which allows the glycerol dehydration to proceed. Although most acid sites were removed from the catalyst by the addition of K, significant amount of the dehydration products (Pathway II and aldehydes) was still obtained. The hydroxyl groups should be partly covered by the alkali metals which suppressed the glycerol dehydration. However, acidic sites of the catalysts should be still remained for the glycerol dehydration to proceed to a minor extent. Also, according to Auroux et al., the conversion of glycerol to acetol can proceed over basic sites of catalysts through either dehydrogenation and consecutive dehydration and hydrogenation, or through dehydration of a terminal hydroxyl group of glycerol to form enol intermediate which can be rapidly rearranged to form acetol [28].

Since it is considered that the Pathway II, the acetol production, and the aldehydes production proceeded through the dehydration of glycerol on acidic sites of catalysts, these reactions were suppressed by the addition of K. On the other hand, it substantially promoted the Pathway I which is the allyl alcohol production. Unlike the formations of acetol and aldehydes, allyl alcohol is assumed to be catalyzed by non-acidic sites of catalysts which should proceed through hydrogen transfer mechanism [12,13]. Schuth et al. and Xu et al. reported acrolein to be an intermediate to allyl alcohol in which acrolein hydrogenates to form allyl alcohol [12,25]. However, based on our investigations this idea is highly unlikely for our reaction system. Firstly, no external hydrogen gas was supplied to our reaction system. Secondly, we conducted the catalytic conversion of pure acrolein aqueous solution over K[5]/ZrO_2–FeO_X and no allyl alcohol was observed in the products as shown in Table 2. Instead, acrolein was mostly converted into the hydrocarbons undetectable by GC with the conversion of 98% which are supposed to be the acrolein polymers.

On the other hand, the hydrogen transfer mechanism to form allyl alcohol possibly takes place in the reactions between glycerol and other intermediates formed during the reaction. To confirm this, we pumped glycerol aqueous solution with acetol, acrolein, acetic acid, or formic acid aqueous solutions through the reactor at *W/F* of 3 h, where *F* is the feed rate of glycerol solution. K[5]/ZrO_2–FeO_X was used as a catalyst. The glycerol conversions and propylene and allyl alcohol yields obtained from glycerol are shown in Table 3. The full glycerol conversions and comparable propylene yields were obtained for all reactions. When acrolein or acetic acid was added to the system, allyl alcohol yield did not increase, which excluded the possibility of the hydrogen transfer reactions between glycerol and acrolein or acetic acid. To be noted, allyl alcohol yield slightly increased when acetol was added and remarkably increased up to 33 mol% C with the addition of formic acid. Formic acid should be formed during the reaction by two possible ways. Firstly, glycerol can dehydrate to form the unstable intermediate 3-hydroxypropionaldehyde (3-HPA). While 3-HPA can further dehydrate to produce acrolein, it can also decompose to obtain acetaldehyde and formaldehyde through a reversed aldol condensation [25]. The follow up oxidation of formaldehyde with the lattice oxygen of FeO_X can give formic acid. Another possible way would be that acetol formed from the glycerol dehydration can oxidatively decompose with the lattice oxygen of FeO_X to give acetic acid and formic acid while acetol can be also isomerized to form propionic acid [29]. Formic acid can further decompose into CO_2 and H_2 over a catalyst and during this catalytic decomposition hydrogen atoms are possibly formed [30]. Therefore, these hydrogen atoms derived from formic acid seem to play an important role in our current reaction system and the

Table 2
Product yields obtained for different model compounds. Reaction conditions: K[5]/ZrO_2–FeO_X, *W/F* = 3 h, reaction time = 2 h.

Model compound (concentration)	Conversion (%)	Product 3 yield (mol% C)									
		Path I		Path II			Aldehydes		Others	Undetectable by GC	CO_2
		Propylene	Allyl Alcohol	Acetol	Carboxylic Acids	Ketones	Acrolein	Acetaldehyde			
Glycerol (30 wt%)	100	0.6	25.4	0.4	3.6	7.4	0.5	3.0	12.2	33.5	13.4
Acrolein (10 wt%)	97.5	0.0	0.0	0.0	0.0	1.2	-	1.2	1.1	89.4	4.6

Table 3
Propylene and allyl alcohol yields for the reactions of glycerol and different intermediates. Reaction conditions: K[5]/ZrO_2–FeO_X, *W/F* = 3 h, reaction time = 2 h.

Feedstock	Glycerol conversion (%)	Product yield (mol% C)	
		Propylene	Allyl alcohol
Glycerol	100	0.6	25.4
Glycerol and acetol	100	1.3	28.4
Glycerol and acrolein	100	1.1	23.6
Glycerol and acetic acid	100	1.0	26.7
Glycerol and formic acid	100	1.1	33.4

The glycerol concentrations were 30 wt% for all reactions. The concentrations of acetol and formic acid aqueous solutions were 30 wt%, and acrolein and acetic acid aqueous solutions were 20 wt%.

hydrogen transfer reaction likely takes place between glycerol and the hydrogen atoms. This well explained the increased allyl alcohol yield with the addition of acetol or formic acid to the system in Table 3.

Another possible mechanism of hydrogen transfer reaction would be the reaction between glycerol and active hydrogen species derived from H_2O molecules. Our previous works consider that ZrO_2–FeO_X has an ability to decompose H_2O molecules into active hydrogen species [22,24]. These active hydrogen species can act as the hydrogen atoms derived from formic acid and play an important role for the formation of allyl alcohol. However, further investigation on a detailed mechanism of the allyl alcohol production is still ongoing in our laboratory.

3.2. Stability of K-supported FeO_X catalyst

The catalytic reaction of 30 wt% glycerol solution was performed for 6 h and *W/F* of 1 h to examine stability of K[5]/ZrO_2–FeO_X. As shown in Fig. 4(a), initial glycerol conversion and allyl alcohol yield were 96% and 26 mol% C, respectively. However, glycerol conversion and allyl alcohol yield drastically decreased to 65% and 14 mol% C with the increase in reaction time. On the other hand, the Pathway II and aldehydes yields maintained approximately 12 mol% C and 7 mol% C, respectively, over 6 h. For the further study of this result, the K content in K[5]/ZrO_2–FeO_X after the catalytic reaction was investigated with an X-ray fluorescence analyzer in our laboratory. It confirmed that the K content still maintained 5 mol% of the total Zr and Fe after the catalytic reaction for 6 h. This well explained the stable yields of the Pathway II and aldehydes over 6 h.

Fig. 5 shows the XRD patterns of K[5]/ZrO_2–FeO_X before and after the reaction. The crystal phase of K[5]/ZrO_2–FeO_X before the reaction was hematite structure. However, that of K[5]/ZrO_2–FeO_X after the reaction for 6 h showed magnetite structure due to the excessive consumption of the lattice oxygen of iron oxide [23,24]. Such change in the crystal phase of the catalyst should be responsible for the reduced catalytic activity and the decreased glycerol conversion and allyl alcohol yield.

In order to maintain high catalytic activity, the suppression of the excessive consumption of the lattice oxygen seems to be beneficial. This could be achieved by calcining the catalyst at higher temperature. However, one controversial point would be that calcination of a catalyst at high temperature may lead to a decrease in surface area of a catalyst [31]. In fact, our investigations showed that the BET surface area of K[5]/ZrO_2–FeO_X drastically decreased from 51 $m^2\,g^{-1}$ to 14 $m^2\,g^{-1}$ with the increase in calcination temperature from 773 K to 973 K, while crystal phase of both catalysts showed hematite structure. This significant decrease in the surface area should result from sintering of FeO_X during calcination. To avoid this negative influence of the higher calcination temperature,

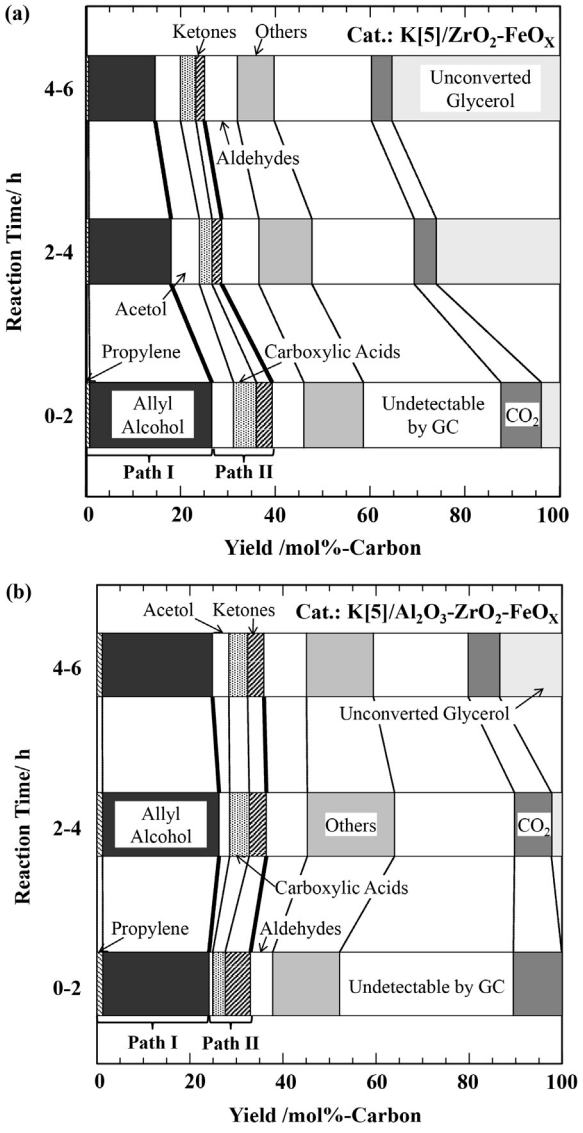

Fig. 4. (a) Stability of K[5]/ZrO_2–FeO_X. Reaction conditions: 30 wt% glycerol solution, K[5]/ZrO_2–FeO_X, *W/F* = 1 h, reaction time = 6 h. (b) Stability of K[5]/Al_2O_3–ZrO_2–FeO_X. Reaction conditions: 30 wt% glycerol solution, K[5]/Al_2O_3–ZrO_2–FeO_X, *W/F* = 3 h, reaction time = 6 h.

Al_2O_3 seems to be the key material since our previous study has revealed that addition of Al_2O_3 to FeO_X was effective in increasing surface area and stability of the FeO_X catalyst for upgrading heavy oil [23,32].

3.3. Characterization and catalytic activity of K[5]/Al_2O_3–ZrO_2–FeO_X

In this study, addition of Al_2O_3 to K/ZrO_2–FeO_X was examined. In consideration of structure stability and surface area of the catalyst, calcining the catalyst at higher temperature and adding Al_2O_3 to the catalyst appears to be advantageous to attain high glycerol conversion and allyl alcohol yield. Therefore, we now developed K[5]/Al_2O_3–ZrO_2–FeO_X.

XRD patterns and BET surface areas of K[5]/ZrO_2–FeO_X and K[5]/Al_2O_3–ZrO_2–FeO_X prior to catalytic reaction are compared in Fig. 5. The crystal phases of both catalysts were hematite structure. Although K[5]/Al_2O_3–ZrO_2–FeO_X was calcined at higher temperature of 973 K, it was shown to have even higher BET surface area (62 $m^2\,g^{-1}$) than K[5]/ZrO_2–FeO_X. This phenomenon is ascribed

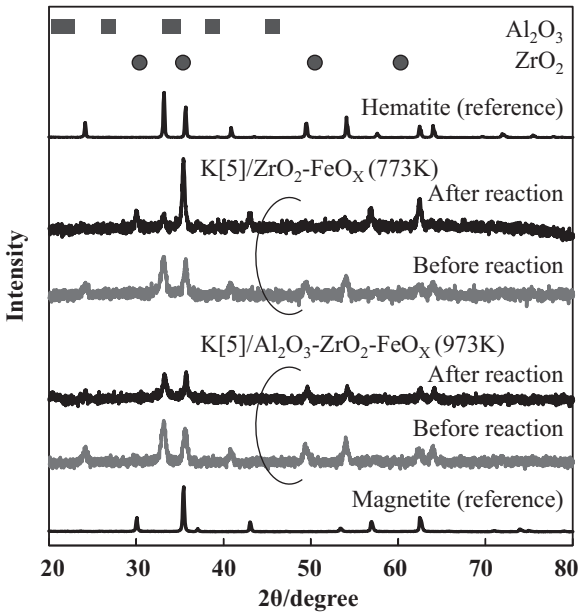

Fig. 5. XRD patterns of K[5]/ZrO_2–FeO_X and K[5]/Al_2O_3–ZrO_2–FeO_X before and after the catalytic reaction. Reaction conditions: 30 wt% glycerol solution, *W/F* = 1 h, reaction time = 6 h.

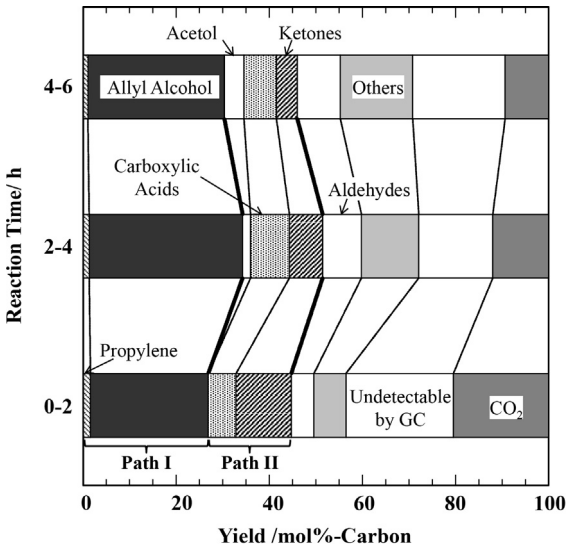

Fig. 6. Catalytic conversion of crude glycerol using K[5]/Al_2O_3–ZrO_2–FeO_X. Reaction conditions: 10 wt% crude glycerol solution, K[5]/Al_2O_3–ZrO_2–FeO_X, *W/F* = 5 h, reaction time = 6 h.

mainly to the addition of Al_2O_3 to K/ZrO_2–FeO_X. Al_2O_3 among the FeO_X crystals suppressed the sintering of the FeO_X and, consequently, high BET surface area of the catalyst was achieved.

Catalytic conversion of 30 wt% glycerol was performed over K[5]/Al_2O_3–ZrO_2–FeO_X. The product yields for K[5]/ZrO_2–FeO_X and K[5]/Al_2O_3–ZrO_2–FeO_X are compared in Fig. 4. As observed in Fig. 4(b), almost no glycerol could be observed in the products for K[5]/Al_2O_3–ZrO_2–FeO_X at the initial reaction period (0–2 h). To our delight, the high glycerol conversion of 87% was attained after 6 h. Allyl alcohol yield also maintained approximately 25 mol% C over 6 h. In general, Al_2O_3 possesses an acid site which would have an effect on the glycerol dehydration. Interestingly, the product yields of the Pathway II and aldehydes for K[5]/Al_2O_3–ZrO_2–FeO_X were 9–11 mol% C and 5–9 mol% C respectively, and these yields were equivalent to those for K[5]/ZrO_2–FeO_X. In K[5]/Al_2O_3–ZrO_2–FeO_X, because K was loaded on Al_2O_3–ZrO_2–FeO_X by an impregnation method, the acidity derived from Al_2O_3 relatively weakened. Accordingly, Al_2O_3 contributed in an impressive increase in surface area and stability of the catalyst without any negative influence on the catalyst acidity. To summarize, K[5]/Al_2O_3–ZrO_2–FeO_X maintained much higher glycerol conversion and allyl alcohol yield over the 6 h reaction compared to K[5]/ZrO_2–FeO_X and showed incredibly higher catalytic stability.

XRD patterns of K[5]/ZrO_2–FeO_X and K[5]/Al_2O_3–ZrO_2–FeO_X after the catalytic conversion for 6 h are shown in Fig. 5. The crystal phase of K[5]/ZrO_2–FeO_X was changed from hematite into magnetite structure after the reaction due to the consumption of the lattice oxygen of iron oxide while K[5]/Al_2O_3–ZrO_2–FeO_X still kept hematite structure. This high structure stability of K[5]/Al_2O_3–ZrO_2–FeO_X well explained the high catalytic stability of the catalyst for allyl alcohol production.

3.4. Catalytic conversion of crude glycerol solution over K[5]/Al_2O_3–ZrO_2–FeO_X

Crude glycerol solution is the waste solution obtained in the process of biodiesel fuel production which contains impurities such as methanol, free fatty acids, ash and water [33]. According to the analysis by a gas chromatograph and an X-ray fluorescence analyzer, crude glycerol was found to consist mainly of glycerol (37 wt%), methanol (8 wt%), potassium (4 wt%), others including free fatty acids (25 wt%), and components undetectable by GC (26 wt%). The crude glycerol was diluted with distilled water and 10 wt% of its solution was used as a feedstock. K[5]/Al_2O_3–ZrO_2–FeO_X was tested for its application for the catalytic conversion of 10 wt% crude glycerol solution at *W/F* of 5 h, where *F* was referred to as the flow rate of the feedstock (g h^{-1}) of crude glycerol solution.

As shown in Fig. 6, useful chemicals such as propylene, allyl alcohol, acetol, carboxylic acids, and ketones were obtained in accordance with the reaction pathways shown in Fig. 1. Although crude glycerol contains impurities, it successfully produced useful chemicals including allyl alcohol over K[5]/Al_2O_3–ZrO_2–FeO_X. Initial allyl alcohol yield was 25 mol% C and its highest yield of 33 mol% C was achieved at the reaction time of 2–4 h. At the reaction

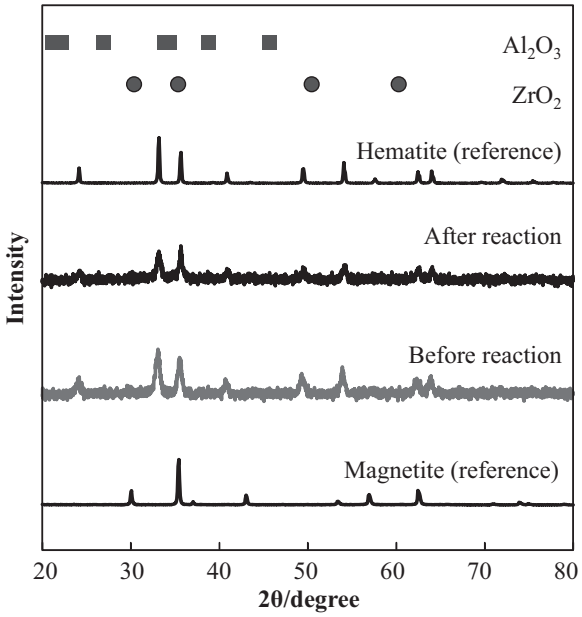

Fig. 7. XRD patterns of K[5]/Al_2O_3–ZrO_2–FeO_X before and after catalytic reaction of crude glycerol. Reaction conditions: 10 wt% crude glycerol solution, *W/F* = 5 h, reaction time = 6 h.

time of 4–6 h the allyl alcohol yield still kept as high as 29 mol% C. The other components in crude glycerol such as free fatty acids and methanol should be degraded during the catalytic reaction. To be noted, the catalyst has the lattice oxygen which can oxidize free fatty acids and methanol into CO_2 and other degraded products. However, these degraded products were not analyzed in this experiment. Thus, they were not included in the product yields in Fig. 6 since the product yields were calculated based on the amount of glycerol fed to the reactor.

Fig. 7 shows XRD patterns of K[5]/Al_2O_3–ZrO_2–FeO_X before and after the catalytic conversion of crude glycerol. The crystal phase of the catalyst before the reaction was hematite structure and the structure was maintained after the reaction. This indicates that the lattice oxygen of FeO_X consumed during the oxidation of free fatty acids and methanol is successfully regenerated by ZrO_2 [23,24]. These results show that K[5]/Al_2O_3–ZrO_2–FeO_X is adequately applicable to the conversion of crude glycerol regardless of its contamination of various impurities.

4. Conclusions

In this work, catalytic conversion of glycerol was performed under nitrogen gas flow with different iron oxide-based catalysts to achieve high allyl alcohol yield. Different alkali metals, including Na, K, Rb, and Cs were supported on ZrO_2–FeO_X with the intent to suppress glycerol dehydration proceeded on the acid sites of the catalyst. All alkali metal-supported ZrO_2–FeO_X gave considerably higher allyl alcohol yield and suppressed glycerol dehydration.

K-supported ZrO_2–FeO_X was selected for further studies regarding allyl alcohol yield. With the increase in K content allyl alcohol yield increased up to 27 mol% C and dehydration products yield drastically decreased. This could be explained by the decreased acidic property of the catalyst by the addition of K. While the glycerol dehydration proceeds on acid sites of catalysts, allyl alcohol is assumed to be produced over non-acidic sites through a hydrogen transfer mechanism. Considering the fact that no external hydrogen is added to the system, the hydrogen transfer mechanism should take place between the reaction of glycerol and either hydrogen atoms derived from formic acid forming during the reaction, or active hydrogen species produced from the decomposition of H_2O by ZrO_2.

To maintain structure stability of the catalyst to obtain higher allyl alcohol yield and glycerol conversion, K[5]/Al_2O_3–ZrO_2–FeO_X was developed. The catalyst was verified to have almost the same surface area and crystal phase with K[5]/ZrO_2–FeO_X. K[5]/Al_2O_3–ZrO_2–FeO_X showed much higher structure stability and maintained remarkably higher allyl alcohol yield of 25 mol% C and glycerol conversion of 87% over 6 h compared to K[5]/ZrO_2–FeO_X without any negative effect on catalyst acidity. Furthermore, K[5]/Al_2O_3–ZrO_2–FeO_X was applicable to the conversion of crude glycerol which is the waste solution obtained from biodiesel production containing impurities such as methanol, free fatty acids, ash, and water. The catalyst maintained the crystal phase of hematite structure over 6 h which indicated the lattice oxygen of FeO_X consumed during the oxidation of free fatty acids and methanol were successfully regenerated by ZrO_2 in the presence of the impurities in crude glycerol.

Acknowledgment

This work was supported by the Industrial Technology Research Grant Programme in 2008, 08B36001c from the New Energy and Industrial Technology Development Organization (NEDO) of Japan.

References

[1] F. Ma, M.A. Hanna, Bioresource Technology 70 (1999) 1–15.
[2] H. Fukuda, A. Kondo, H. Noda, Journal of Bioscience and Bioengineering 92 (2001) 405–416.
[3] L.C. Meher, D.V. Sagar, S.N. Naik, Renewable and Sustainable Energy Reviews 10 (2006) 248–268.
[4] A. Behr, J. Eilting, K. Irawadi, J. Leschinski, F. Lindner, Green Chemistry 10 (2008) 13–30.
[5] S.H. Chai, H.P. Wang, Y. Liang, B.Q. Xu, Journal of Catalysis 250 (2007) 342–349.
[6] E. Tsukuda, S. Sato, R. Takahashi, T. Sodesawa, Catalysis Communications 8 (2007) 1349–1353.
[7] A. Corma, G.W. Huber, L. Sauvanaud, P. O'Connor, Journal of Catalysis 257 (2008) 163–171.
[8] S. Sato, M. Akiyama, R. Takahashi, T. Hara, K. Inui, M. Yokota, Applied Catalysis A-General 347 (2008) 186–191.
[9] T. Miyazawa, S. Koso, K. Kunimori, K. Tomishige, Applied Catalysis A-General 329 (2007) 30–35.
[10] D.G. Lahr, B.H. Shanks, Journal of Catalysis 232 (2005) 386–394.
[11] T. Kurosaka, H. Maruyama, I. Naribayashi, Y. Sasaki, Catalysis Communications 9 (2008) 1360–1363.
[12] Y. Liu, H. Tuysuz, C.J. Jia, M. Schwickardi, R. Rinaldi, A.H. Lu, W. Schmidt, F. Schuth, Chemical Communications 46 (2010) 1238–1240.
[13] J. Yi, S. Liu, M.M. Abu-Omar, ChemSusChem 5 (2012) 1401–1404.
[14] M. Shiramizu, F.D. Toste, Angewandte Chemie International Edition 51 (2012) 8082–8086.
[15] L. Qadariyah, Mahfud, Sumarno, S. Machmudah, Wahyudiono, M. Sasaki, M. Goto, Bioresource Technology 102 (2011) 9267–9271.
[16] T. Masuda, Y. Kondo, M. Miwa, T. Shimotori, S.R. Mukai, K. Hashimoto, M. Takano, S. Kawasaki, S. Yoshida, Chemical Engineering Science 56 (2001) 897–904.
[17] D. Na-Ranong, R. Yuangsawad, T. Tago, T. Masuda, Korean Journal of Chemical Engineering 25 (2008) 426–430.
[18] T. Yoshikawa, D. Na-Ranong, T. Tago, T. Masuda, Journal of the Japan Petroleum Institute 53 (2010) 178–183.
[19] D. Mansur, T. Yoshikawa, K. Norinaga, J. Hayashi, T. Tago, T. Masuda, Fuel 103 (2013) 130–134.
[20] E. Fumoto, Y. Mizutani, T. Tago, T. Masuda, Applied Catalysis B: Environmental 68 (2006) 154–159.
[21] S. Funai, Y. Satoh, Y. Satoh, K. Tajima, T. Tago, T. Masuda, Topics in Catalysis 53 (2010) 654–658.
[22] T. Yoshikawa, T. Tago, A. Nakamura, A. Konaka, M. Mukaida, T. Masuda, Research on Chemical Intermediates 37 (2011) 1247–1256.
[23] S. Funai, E. Fumoto, T. Tago, T. Masuda, Chemical Engineering Science 65 (2010) 60–65.
[24] E. Fumoto, T. Tago, T. Tsuji, T. Masuda, Energy Fuels 18 (2004) 1770–1774.
[25] S.H. Chai, H.P. Wang, Y. Liang, B.Q. Xu, Green Chemistry 9 (2007) 1130–1136.
[26] W. Suprun, M. Lutecki, T. Haber, H. Papp, Journal of Molecular Catalysis A: Chemical 309 (2009) 71–78.
[27] K. Pathak, M. Reddy, N.N. Bakhshi, A.K. Dalai, Applied Catalysis A-General 372 (2010) 224–234.
[28] D. Stosic, S. Bennici, J.L. Couturier, J.L. Dubois, A. Auroux, Catalysis Communications 17 (2012) 23–28.
[29] D.J. Hopper, E.A. Elmorsi, Biochemical Journal 218 (1984) 269–272.
[30] I. Gandarias, P.L. Arias, S.G. Fernandez, J. Requies, M.E. Doukkali, M.B. Guemez, Catalysis Today 195 (2012) 22–31.
[31] J.M. Jehng, I.E. Wachs, Journal of Molecular Catalysis 81 (1993) 63–75.
[32] E. Fumoto, T. Tago, T. Masuda, Energy Fuels 20 (2006) 1–6.
[33] M. Ayoub, A.Z. Abdullah, Renewable and Sustainable Energy Reviews 16 (2012) 2671–2686.